Eur. Phys. J. D **45**, 433–437 (2007)
DOI: 10.1140/epjd/e2007-00213-7

THE EUROPEAN PHYSICAL JOURNAL D

The structure of cobalt nanoparticles on Ge(001)

K. Sell[a], A. Kleibert, V. v. Oeynhausen, and K.-H. Meiwes-Broer

University of Rostock, Department of Physics, Universitätsplatz 3, 18051 Rostock, Germany

Received 20 February 2007 / Received in final form 3 May 2007
Published online 27 June 2007 –

Abstract. In this contribution we present scanning tunnelling microscopy (STM) and spectroscopy (STS) investigations on isolated cobalt clusters in contact with Ge(001). Mass-filtered nanoparticles with diameters ranging from 3 to 11 nm are generated using an arc cluster ion source (ACIS) and deposited under soft landing conditions (E_{kin}/atom < 0.5 eV). Since the tip radius is of the same order as the nanoparticle diameters the recorded STM images are significantly affected by tip folding. By means of the "blind reconstruction method" it is possible to approximate the tip shape. After a respective deconvolution of the image structural features of the particle facets become observable. According to the equilibrium shape of the clusters being a truncated octahedron in the size range under investigation, hexagonal and rectangular features appear in the images. STS is sensitive to occupied and unoccupied states near the Fermi level and reveals the existence of distinct states in the tunnelling conductivity of the substrate as well as on the clusters. The richly structured density of states of the germanium surface serves here as tip condition test. First measurements of the tunnelling conductivity of the Co_N/Ge(001) are presented and discussed.

PACS. 68.37.Ef Scanning tunneling microscopy – 61.46.Df Nanoparticles – 61.46.Bc Clusters

1 Introduction

Clusters and nanoparticles are intermediate systems allowing for investigations on the evolution from atomic to bulk matter properties. Since the transition from a single atom to the respective solid occurs strongly non-linear clusters usually show remarkable and size-dependent modifications of their electronic, structural as well as their magnetic properties [1–3]. In the case of cobalt the cluster properties are mainly governed by their $3d$ electrons. In particular the narrowing of the $3d$ bands due to the reduced coordination of surface atoms results in strongly enhanced magnetic moments in small clusters as observed in Stern-Gerlach experiments [4]. From these experiments on free particles it turned out that bulk-like magnetic properties are already recovered for clusters consisting of more than approximately 500 atoms. However, recent experiments on much larger particles after deposition onto epitaxially ordered surfaces revealed bulk-like spin but remarkably enhanced magnetic orbital moments [5–7]. Furthermore a significant dependence on the substrate material has been observed that hints towards a sizable cluster substrate interaction. The underlaying complex interplay of structure, shape and interface energies still has to be resolved. Part of the present study thus aims at an in situ investigation on the geometric structure and shape of deposited cobalt nanoparticles.

[a] e-mail: kristian.sell@uni-rostock.de

In bulk, Co is known to exhibit hcp and fcc structure with a transition temperature of about 694 K. The electronic and geometric structure of solid cobalt is well known [8,9]. For nanoparticles the crystalline structure depends on their size. Kitakami et al. [10] showed that Co particles below 20 nm diameter form a fcc structure (β-cobalt), up to 30 nm a mixed crystal and above 40 nm a hcp structure (α-cobalt). Calculations [11] predict an icosahedrical shape for an atom number N ranging from 4 to 60 atoms. In experiments a β-Wulff-polyhedron was observed in the size range from 6 to 110 nm [12]. The shape of this truncated octahedron minimizes the free surface energy and switches to a metastable β-multiply-twined icosahedron below 6 nm diameter. At high temperatures this shape relaxes to the β-Wulff-polyeder.

The electronic structure of the solid Co(0001) surface was investigated by Himpsel et al. [13]. Photoelectron spectroscopy showed a number of dominant states near the Fermi level. In particular the state near -300 meV can also be found in STS studies of Wiebe et al. [14] for thin Co(0001) films ranging from 4 to 10 ML. This spectral feature was interpreted as a surface state. Okuno et al. [15] observe a spin-polarized surface state in this range (near -0.43 eV) by tunneling experiments prepared on 4 to 8 nm thick Co-films. They interpreted it as a minority spin Γ-centered d_z^2-like surface state. STS-investigations by Morgenstern et al. [16] on cobalt islands on InAs(110) also provide evidence for this state,

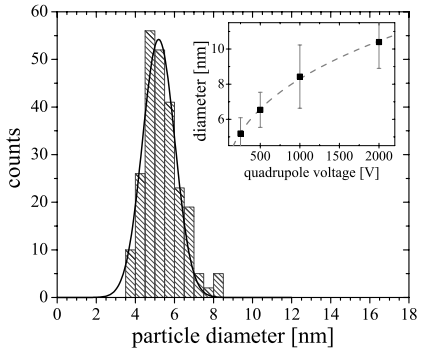

Fig. 1. Example of a Co particle size distribution from a deposition investigated by TEM. Inset: the size distribution can be shifted by adjusting the quadrupole voltage (dots: as measured, dashed line: calculated).

whereas Pratzer et al. [17] observed structure-dependent differences in the tunnelling conductance of fcc and hcp films. Nanoparticles prepared by atomic evaporation on a Pt(111)-surface were investigated by Rusponi et al. [18] with spin-polarized STM. They observed tunnelling into spin-polarized surface states which are responsible for the increased vacuum tunnelling magnetoresistance [19].

In the here presented investigations cobalt particles are prepared in a size range from 3 to 15 nm and deposited from a beam onto a Ge(001) surface. The combination of high DOS Co with the semiconducting Ge should lead to interesting tunnelling properties which we will investigate by STS.

2 Experimental

The cobalt clusters are produced with a continuous Arc Cluster Ion Source (ACIS) [20] directly connected to the preparation chamber so that the particles can be deposited under UHV conditions on a cleaned substrate. The cluster source has been developed to produce a high flux of mass filtered metal clusters in the size range of about 3 to 15 nm. The size selection of the charged particles is achieved by a 90°-deflection in the electrical field of an electrostatic quadrupole. The beam flux can be estimated from the cluster ion current during deposition. An undoped Ge(001) wafer material fixed to a tungsten sample holder is used as substrate. To clean the germanium a moderate heating followed by sputtering-heating cycles is performed until LEED observations show a clean crystalline surface. The sputtering process lasts for some minutes with a high-voltage of about 850 eV (argon or neon, about 3 μA sputtering current) and is followed by a short flash up to 1070 K. At room temperature one could observe the p(2 × 1) reconstruction pattern with LEED whereas at low temperatures (lN2) the two reconstructions p(2×2) and c(4×2) coexist on the germanium surface [21].

Investigations with Transmission Electron Microscopy (TEM) provide size distributions of the produced particles. As an example Figure 1 depicts such a distribution of the clusters selected by a quadrupole voltage of 250 V with a resulting average diameter of 5.3 nm ± 1.0 nm. With the setting of the quadrupole voltage (Inset in Fig. 1) mean diameters can be chosen from 3 to 15 nm, i.e. 1500 to 150000 atoms.

The tunnelling microscopy and spectroscopy is performed with a Low Temperature - Scanning Tunnelling Microscope (LT-STM) from Omicron Nanotechnology. The base pressure in the analysis chamber is about 2×10^{-11} mbar. For the STM investigations tungsten tips are used that were chemically etched and heated in the UHV. For testing the tip quality the known germanium tunnelling conductance spectra can be used. All the here presented measurements are performed at a temperature of about 80 K. Tunnelling conductance is investigated by $I(V)$ measurements. Additionally the signal can directly be processed by a lock-in amplifier. In that case a reference signal with about 400 Hz and an amplitude below 10 mV rms is used.

3 Results

In TEM observations (Figs. 2a–2c) the clusters show in principal a spherical shape. With high resolution TEM (HRTEM) the atomic structure of the particles can be resolved. In Figure 2c two connected Co nanoparticles are recorded with atomic resolution. Here first evidences appear hinting at different types of facets — rectangular and hexagonal shapes. From STM measurements we determine the cluster heights. This measurement can be affected by the change of the density of states from the semiconducting substrate to the metallic cluster. In the work of Hövel and Barke [22] the dependence of measured Au_N/HOPG heights on the tunnelling voltage was demonstrated. With respect to these observations we expect an error smaller than 10% for the here discussed particle heights.

When comparing the particle diameters obtained from TEM with height measurements by STM the TEM results show larger diameters when compared to the measured heights. This difference could have two reasons. One is the oxidation of the particles while being transported to the TEM which results in a systematical error of about 1 nm in the size distributions. Second, the interaction of the particles with the germanium might lead to a flattening. Comparing measured heights with diameters we deduce an aspect ratio of 1.2. Obviously the cobalt clusters do not significantly change their shape upon deposition since this ratio is close to 1. In contrast, in a corresponding work on silver clusters on Ge(001) we found and aspect ratio of about 2 [23].

Due to the fact that the radius of the STM tip is in the range of about 3 nm one has to anticipate strong convolution effects of tip and sample topography when imaging such large particles. As one can see in Figure 3 the tip shape dominates in the raw image of the sample topography. In such a case we are able to approximate the tip shape from the sample image with the help of the "blind reconstruction" method described by Villarrubia [24,25] and Williams et al. [26]. Once the shape is found its influence can partly be deconvoluted from the sample image.

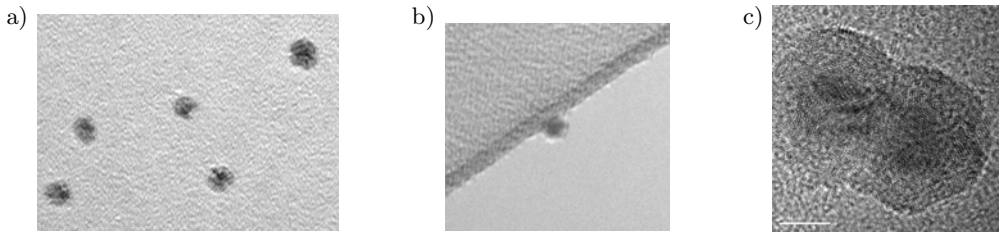

Fig. 2. TEM images of cobalt clusters. (a) Top view (144 nm × 103 nm), (b) side view (72 nm × 66 nm), (c) high resolution TEM (23 nm × 23 nm) of two connected particles. All particles appear principally spherical.

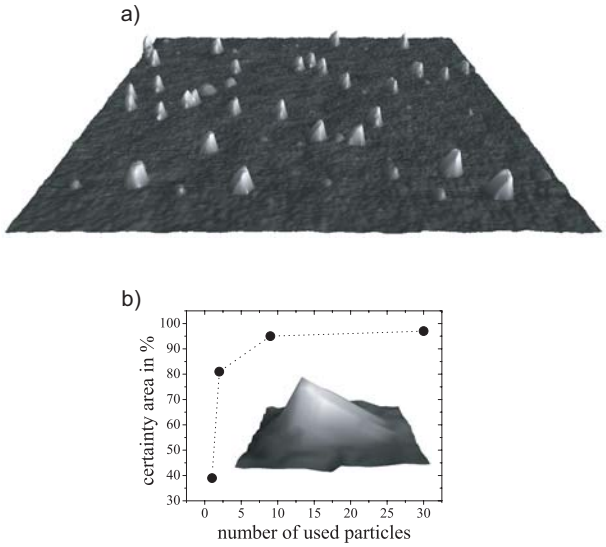

Fig. 3. (a) STM topography (500 nm × 500 nm, $U_t = 0.15$ V, $I_t = 0.15$ nA) of Co particles (heights about 5 nm) deposited on a Ge(001) substrate (raw data). The strong tip convolution is superimposed on the individual cluster shapes. (b) Certainty area during the deconvolution process versus number of included particles. Inset: a tip shape reconstructed from the topography of Figure 3a.

The blind reconstruction method is based on the operations of the mathematical morphology. It determines, not knowing anything about the sample topography, the set of points in the image that are common to all objects (here: clusters). With this information the algorithm approximates a shape of the tip. For a successful approximation one has to include a certain amount of objects. Figure 3b shows the relation of the number of included objects and the certainty of the tip characterization. Here it was possible to get a certainty above 90% with only 10 particles. In principle the number of test objects necessary depends on the ratio of tip radius to the cluster diameter. As a result of the deconvolution process information of the cluster shape can be obtained. Note, however, that the lateral extension cannot be reproduced reliably due to a nonreconstructable area in the surrounding of each particle. The asymmetric "shadows" particularly on the left side of the clusters are an artefact of the feedback loop of the STM system. The number of data points per object is also an important parameter for this method. Here it is just sufficient to perform a reasonable tip deconvolution.

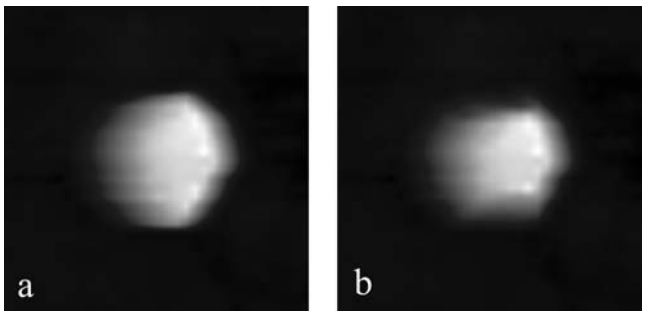

Fig. 4. Comparison of (a) the raw data and (b) the tip deconvoluted image of a cluster (50 nm × 50 nm).

With less points it is hardly possible to decide whether the seen features are real or just an artefact of the low data resolution. The result of the mathematically processed deconvoluted image in Figure 3a is shown in Figure 5a. The marked particles are magnified in Figure 5b. They feature hexagonal, triangular and nearly rectangular shapes. Figure 4 shows a comparison between (a) the raw data and (b) the tip deconvoluted image of a single cluster. As it can be seen in Figure 4a the raw data gives a first impression of the particle shape. With tip deconvolution it is possible to highlight these features. We see no reason why such features should be induced by the "blind reconstruction method". Neither a symmetry related to the scan process nor any process used in the algorithm can explain the various observed particle shapes and orientations.

As expected from thermodynamical consideration the here investigated Co clusters should have the shape of a β-Wulff polyhedron which is a truncated octahedron. The particle shapes observed after tip deconvolution (Fig. 5) are in agreement with the expectation. They exhibit the characteristical hexagonal and rectangular features of truncated octahedra which were differently orientated by deposition. This supports also the results of Kitakami et al. [10] for the fcc-structured particles in the size range below 20 nm. Furthermore we observe some nearly triangular shaped systems (Fig. 5 left, 1). According to Kitakami et al. [10] this may probably indicate that some of the produced nanoparticles have hcp structure and form Wulff polyhedra of α-cobalt. The indication for α-cobalt cannot be ruled out based on our STM data although they unlikely appear for particles smaller 30 nm.

First investigations of the tunnelling conductance were performed with the help of STS. In Figure 6a I–V-curves

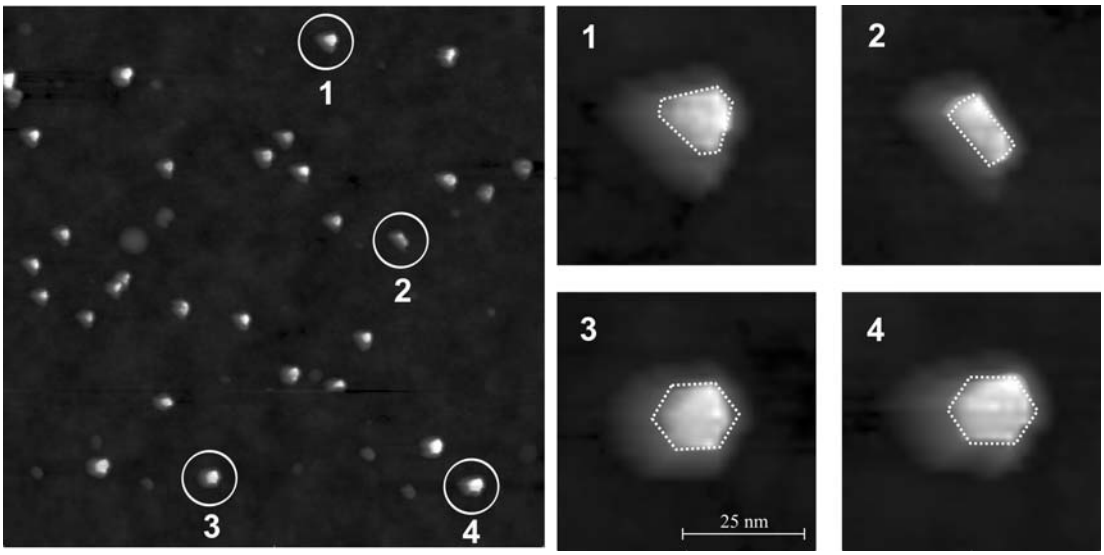

Fig. 5. Deconvoluted STM topography (500 nm × 500 nm, U_t = 0.15 V, I_t = 0.15 nA) of Figure 3a. On the right side the clusters marked in the overview are shown magnified. Size of the images is 50 nm × 50 nm (interpolated).

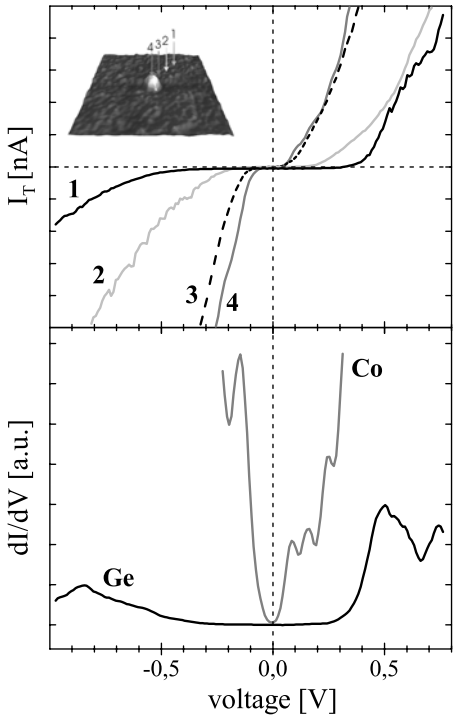

Fig. 6. Top: tunnelling current versus bias voltage (open feedback) measured from the germanium substrate to the center of the cobalt cluster. Bottom: tunnelling conductance measured on the germanium compared to a measurement performed on top of a cobalt particle.

are shown where the lateral distance to the middle of the particle was varied. Curve 1 shows the expected gap for the measurement on the pure germanium substrate. In previous investigations we determined this gap in the electronic surface state structure of Ge(001) to about 250 meV [23]. With decreasing lateral distance of the measurement position to the cluster (inset in Fig. 6a) the gap width also decreases and the slope of the curve increases — the behaviour gets more metallic.

Corresponding STS spectra making use of the lock-in technique are shown in Figure 6b. The tunnelling conductance and therefore the electronic density of states near the Fermi level is distinctly higher for the cluster than for the substrate (Fig. 6b). With negative bias (occupied states) many spectra exhibit a distinct peak around −200 to −400 meV. That feature might be related to the repeatedly described surface state [15,16] of cobalt films and cobalt nanoparticles.

In conclusion, mass filtered Co nanoparticles have been deposited from a beam onto Ge(001). By means of the "blind reconstruction" method it becomes possible to partially resolve details of the particle shapes that are in agreement with the β-Wulff polyhedron equilibrium shape for cobalt cluster. First tunnelling experiments show dramatic differences between the metal and the underlaying semiconductor. In future STS will be used as a very sensitive method to investigate the electronic structure of single cluster facets.

We thank the Deutsche Forschungsgemeinschaft for financial support within the SPP 1153 and the EMZ Rostock for the possibility to use the TEM.

References

1. *Clusters of atoms and molecules*, edited by H. Haberland (Springer, 1994)
2. U. Kreibig, M. Vollmer, *Optical properties of metal clusters* (Springer, 1995)
3. *Clusters on Surfaces*, edited by K.-H. Meiwes-Broer (Springer, 2000)
4. I.M.L. Billas, A. Chatelain, W.A. de Heer, Science **265**, 1682 (1994)

5. J. Bansmann, M. Getzlaff, A. Kleibert, F. Bulut, R.K. Gebhardt, K.H. Meiwes-Broer, Appl. Phys. A **82**, 73 (2006)
6. J. Bansmann, A. Kleibert, Appl. Phys. A **80**, 957 (2005)
7. J. Bansmann et al., Surf. Sci. Rep. **56**, 189 (2005)
8. F. Batallan, I. Rosenman, C.B. Sommers. Phys. Rev. B **11**, 545 (1975)
9. S. Wakoh, J. Yamashita, J. Phys. Soc. Jpn **28**, 1151 (1970)
10. O. Kitakami, H. Sato, Y. Shimada, F. Sato, M. Tanaka, Phys. Rev. B **56**, 13849 (1997)
11. J.L. Rodriguez-Lopez, F. Aguilera-Granja, K. Michaelian, A. Vega, Phys. Rev. B **67**, 174413 (2003)
12. M. Jamet, W. Wernsdorfer, C. Thirion, D. Mailly, V. Dupuis, P. Melinon, A. Perez, Phys. Rev. Lett. **86**, 4676 (2001)
13. F.J. Himpsel, D.E. Eastman, Phys. Rev. B **20**, 3217 (1979)
14. J. Wiebe, L. Sacharow, A. Wachowiak, G. Bihlmayer, S. Heinze, S. Blügel, M. Morgenstern, R. Wiesendanger, Phys. Rev. B **70**, 035404 (2004)
15. S.N. Okuno, T. Kishi, K. Tanaka, Phys. Rev. Lett. **88**, 066803 (2002)
16. M. Morgenstern, J. Wiebe, A. Wachowiak, M. Getzlaff, J. Klijn, L. Plucinski, R.L. Johnson, R. Wiesendanger, Phys. Rev. B **65**, 155324 (2002)
17. M. Pratzer, H.J. Elmers, Phys. Rev. B **72**, 035460 (2005)
18. S. Rusponi, N. Wiess, T. Cren, M. Epple, H. Brune, Appl. Phys. Lett. **87**, 162514 (2005)
19. R. Wiesendanger, M. Bode, M. Getzlaff, Appl. Phys. Lett. **75**, 124 (1999)
20. R.P. Methling, V. Senz, E.D. Klinkenberg, Th. Diederich, J. Tiggesbäumker, G. Holzhüter, J. Bansmann, K.H. Meiwes-Broer, Eur. Phys. J. D **16**, 173 (2001); J. Bansmann, M. Getzlaff, A. Kleibert, F. Bulut, R.K. Gebhardt, K.H. Meiwes-Broer, Appl. Phys. A **82**, 73 (2006)
21. W. Ernst, K.-L. Jonas, V. von Oeynhausen, C. Tegenkamp, H. Pfnür, Phys. Rev. B **68**, 205303 (2003)
22. H. Hövel, I. Barke, Progr. Surf. Sci. **81**, 53 (2006)
23. K.-L. Jonas, V. von Oeynhausen, J. Bansmann, K.-H. Meiwes-Broer, Appl. Phys. A **82**, 131 (2006)
24. J.S. Villarrubia, Surf. Sci. **321**, 287 (1994)
25. J.S. Villarrubia, J. Res. Natl. Inst. Stand. Technol. **102**, 425 (1997)
26. P.M. Williams, K.M. Shakesheff, M.C. Davies, D.E. Jackson, C.J. Roberts, S.J.B. Tendler, J. Vac. Sci. Technol. B **14/2**, 1557 (1996)